Limnologica 59 (2016) 90–98

Contents lists available at ScienceDirect

Limnologica

journal homepage: www.elsevier.com/locate/limno

The fate of C_4 and C_3 macrophyte carbon in central Amazon floodplain waters: Insights from a batch experiment

J.M. Mortillaro[a,i,*], C. Passarelli[a], G. Abril[b,c], C. Hubas[a], P. Alberic[d], L.F. Artigas[e], M.F. Benedetti[f], N. Thiney[a], P. Moreira-Turcq[g], M.A.P. Perez[c,f], L.O. Vidal[h], T. Meziane[a]

[a] *Unité Mixte de Recherche Biologie des organismes et écosystèmes aquatiques (BOREA UMR 7208), Sorbonne Université, Muséum national d'Histoire naturelle, Université Pierre et Marie Curie, Institut de Recherche pour le Développement, Université de Caen Basse-Normandie, Université des Antilles, Paris, France*

[b] *Laboratoire Environnements et Paléoenvironnements Océanique (EPOC) UMR-CNRS 5805, Université de Bordeaux, Allée Geoffroy Saint-Hilaire 33615 Pessac, France*

[c] *Universidade Federal Fluminense, Department of Geochemistry, Niteroi, Rio de Janeiro, Brazil*

[d] *Institut des Sciences de la Terre d'Orléans, 1A rue de la Férollerie, 45071 Orléans Cedex 2, France*

[e] *Laboratoire d'Océanologie et Géosciences (LOG), UMR-CNRS-ULCO-UL1 8187, Université du Littoral Côte d'Opale (ULCO), 32 avenue Foch, 62930 Wimereux, France*

[f] *Equipe Géochimie des Eaux, Institut de Physique du Globe de Paris, Université Paris Diderot, Sorbonne Paris Cité, 35 rue Hélène Brion, 75205 Paris Cedex 13, France*

[g] *Institut de Recherche pour le Développement, (IRD)—GET, Lima, Peru*

[h] *Laboratório de Ecologia Aquática, Departamento de Biologia, Universidade Federal de Juiz de Fora, Rua José Lourenço Kelmer, MG 36036-900 Juiz de Fora, Brazil*

[i] *CIRAD, UMR 116 ISEM, Institut de Recherche pour le Développement, TA B116/16, Montpellier, France*

ARTICLE INFO

Article history:
Received 15 May 2015
Received in revised form 1 March 2016
Accepted 6 March 2016
Available online 17 May 2016

Keywords:
Central amazon
Floodplains
Fatty acids
Stables isotopes
Macrophytes
Degradation

SUMMARY

The central Amazon floodplains are particularly productive ecosystems, where a large diversity of organic carbon sources are available for aquatic organisms. Despite the fact that C_4 macrophytes generally produce larger biomasses than C_3 macrophytes, food webs in the central Amazon floodplains appear dominantly based on a C_3 carbon source.

In order to investigate the respective fate and degradation patterns of C_4 and C_3 aquatic plant-derived material in central Amazon floodplains, we developed a 23-days batch experiment. Fatty acid and carbon concentrations as well as stable isotope compositions were monitored over time in 60 L tanks. These tanks contained Amazon water, with different biomasses of C_3 and C_4 macrophyte, representative of in situ densities occurring in central Amazon floodplains.

In the C_4 *Paspalum repens* treatments, organic (POC, DOC) and inorganic carbon (DIC) got rapidly enriched in ^{13}C, whereas in the C_3 *Salvinia auriculata* treatments, POC and DOC showed little change in concentration and isotopic composition, and DIC got depleted in ^{13}C. The contribution of *P. repens* to POC and DOC was estimated to reach up to 94.2 and 70.7%, respectively. In contrast, no differences were reported between the C_3 *S. auriculata* and control treatments, an observation attributed to the lower C_3 biomass encountered in the field, to a slower degradation rate of C_3 compared to C_4 compounds, and to similar isotopic compositions for river POC and DOC, and C_3 compounds.

The ^{13}C enrichments of POC, DOC, and DIC from *P. repens* treatments were attributed to an enhanced bacterially-mediated hydrolysis and mineralization of C_4 material. Evolutions of bacterial abundance and branched fatty acid concentrations confirmed the role of heterotrophic microbial communities in the high *P. repens* decomposition rate. Our experiment highlights the predominant role of C_4 aquatic plants, as a large source of almost entirely biodegradable organic matter available for heterotrophic activity and CO_2 outgassing to the atmosphere.

1. Introduction

One of the largest sources of organic carbon in Amazon floodplains is derived from aquatic macrophytes, which contribute up

* Corresponding author.
E-mail address: jean-michel.mortillaro@cirad.fr (J.M. Mortillaro).

http://dx.doi.org/10.1016/j.limno.2016.03.008
0075-9511/

Fig. 1. Floating meadows of *P. repens* (left) and *S. auriculata* (right).

to half of the ecosystem primary production (Melack and Forsberg, 2001). These macrophytes grow emerged, submerged or floating, with 388 species described in a várzea (i.e. white-water nutrient rich floodplain) located near the city of Manaus, in central Amazon (Junk and Piedade, 1993b). Among the most abundant species, the floating grasses *Echinochloa polystachya* and *Paspalum fasciculatum* (Poaceae family) can reach biomasses of 80 and 60 t ha^{-1}, respectively (Junk and Piedade, 1993a; Piedade et al., 1991). Another macrophyte largely represented in the várzea is *P. repens* (up to 22 t ha^{-1}, Fig. 1, Junk and Piedade, 1993a). These aerial species, which convert atmospheric carbon dioxide into biomass through a C_4 pathway, constitute floating meadows that can extend over large areas of floodplains (Junk and Howard-Williams, 1984; Hess et al., 2003; Silva et al., 2013). Amazon floating meadows may also be composed of macrophytes using the C_3 photosynthetic pathway such as *Eichhornia* sp., *Pistia stratiotes* and *Salvinia auriculata* (Fig. 1). However, the biomass of all these C_3 macrophytes add up to 3–15 t ha^{-1} only (Furch and Junk, 1992).

The ecology of C_3 and C_4 macrophytes, and particularly their biomass and production rates, have been thoroughly examined (e.g. Morison et al., 2000; Engle et al., 2008; Silva et al., 2013). Despite their large abundance, C_4 macrophytes constitute a minor source of energy for Amazon aquatic food webs (Hamilton et al., 1992; Forsberg et al., 1993; Mortillaro et al., 2015) and modest contributors to particulate organic carbon (POC, Hedges et al., 1986; Mortillaro et al., 2011; Moreira-Turcq et al., 2013). Indeed, C_4 macrophytes are largely ^{13}C enriched (−12‰, Hedges et al., 1986; Mortillaro et al., 2011) compared to POC in rivers and várzea of the Amazon (−30‰, Quay et al., 1992; Hedges et al., 1994). The almost constant isotopic composition of dissolved organic carbon (DOC), at around −29‰ in the Amazon River, suggests a dominant C_3 source such as terrestrial plants and/or macrophytes. In contrast, dissolved inorganic carbon (DIC) is much heavier (−17.7 to −11.5‰, Quay et al., 1992), i.e. closer to C_4 macrophytes signature, but also closer to the signature of atmospheric CO_2. This isotopic composition results from isotopic equilibration induced by CO_2 gas exchange (Quay et al., 1992; Hedges et al., 1994; Mayorga et al., 2005; Abril et al., 2014), and/or due to carbonate mineral weathering (e.g. chemical or mechanical decay of rocks, Mayorga et al., 2005).

Previous macrophyte (C_3 and C_4) degradation experiments in litterbags, exposed to natural weathering, found an initially rapid loss of weight and a decrease in nutrients (Howard-Williams and Junk, 1976; Furch and Junk, 1992). However, the contribution of macrophytes to the Amazon aquatic food webs was not verified by Fellerhoff et al. (2003) in their degradation experiment. Therefore, in order to examine the apparent discrepancy between the high biomass of C_4 macrophytes in the floodplains and their modest contribution to the organic matter (OM) pool in the Amazon river-floodplain ecosystem, a degradation experiment was designed to investigate the fate of carbon from C_4 and C_3 macrophytes in microcosms. Particulate and dissolved carbon concentrations, stable isotope compositions and fatty acids (FA) concentrations, were analyzed in large volumes of Amazon waters incubated with variable amounts of a C_4 and a C_3 macrophyte. Bacterial abundance and nutrient concentrations complemented the description of macrophyte degradation throughout a 23-day experiment. Our work hypothesis was that very fast decomposition and mineralization of C_4 macrophytes explain their low contribution to central Amazon aquatic food webs.

2. Material and methods

2.1. Sampling

In order to follow the fate of OM during the degradation of two aquatic macrophytes and the influence of degradation products on the quality of POM, samples of *P. repens* (C_4) and *S. auriculata* (C_3, Fig. 1) were collected in the Camaleão Lake (várzea), located by the Solimões River. These two macrophytes were selected for their widespread distribution in central Amazon floodplains and their large FA concentration compared to other macrophyte species (i.e. *Eichhornia* sp. and *Pistia stratiotes*), as characterized in a previous study (Mortillaro et al., 2011).

Macrophyte samples were sorted in order to eliminate dead leaves and washed to remove sediment and invertebrates. About 900 L of water were also sampled from the lake and distributed into 15 microcosms of 60 L each. Three water samples and three portions of each macrophyte were collected in order to get their initial composition (i.e. stable isotopes and FA).

2.2. Experimental setup

The experiment was implemented on the *Yane José IV* boat in August-September 2010. Five experimental treatments were used: high and low biomasses of *P. repens* (PR-HB and PR-LB, respectively) and *S. auriculata* (SA-HB and SA-LB, respectively), as well as a control without macrophyte (Ctrl). These five treatments were selected

to distinguish species effect from biomass effect on water characterization. For each treatment, triplicate microcosms were used. In PR-HB microcosms, 250 g of fresh *P. repens* leaves (25.6 gC) were used. This amount was estimated from a maximum dry biomass of 22 t ha^{-1} (recorded in the Janauari Lake near Camaleão Lake, Junk and Piedade, 1993a), with less than one fifth of emerged *P. repens* biomass (Silva et al., 2009), an estimated water proportion of 75.9% and a microcosms surface of 0.13 m^2. Similarly, the mean *S. auriculata* dry biomass was estimated to be 1 t ha^{-1} (Junk and Piedade, 1997) giving a theoretical wet weight of 200 g (93.5% of water). However, low biomasses of *S. auriculata* were available during sampling, so that only 100 g (2.3 gC) per microcosm were used (SA-HB). Low biomass treatments contained 10% of the high biomass amount for each species (25 g of macrophytes for PR-LB and 10 g for SA-LB). Macrophyte leaves were introduced into microcosms filled with floodplain water, and were kept in the dark under constant temperature conditions (28 °C). Permanent stirring with a water pump ensured oxygenation of the microcosms (from 40 to 100% air-saturation) and avoided anaerobic conditions to occur. Although low dissolved oxygen is common under floating macrophytes in várzea (~50% saturation, Engle and Melack, 1993), permanent oxygenation was maintained in order to match natural conditions within floating meadows in open waters, where wind and water currents are sufficient to maintain aerated to hypoxic waters (30% min) in 2–6 m depth water column (Vidal et al., 2015).

In each treatment, samples were collected after 3, 6, 12, 18 and 23 days of experiment. At each sampling time, around 3.5 L of water were collected and pre-filtered on 200 μm to avoid heterogeneity between samples due to contamination with macrophyte fragments. Consequently, POC concentrations reported here concern the fraction smaller than 200 μm. Microcosms volume (60 L) was chosen so that at the end of the experiment, 70% of the initial water volume was still available, to avoid any concentration bias in the course of the experiment.

2.3. Sample analyses

The FA compositions of POM and macrophytes were analyzed with a gas chromatograph (Varian CP-3800 with flame ionization detector) after extraction, following a modified method of Bligh and Dyer (1959) as described in Mortillaro et al. (2011). POM samples were obtained after immediate on-board filtration (GF/F, 0.7 μm, pre-combusted 12 h at 450 °C) using a vacuum system under low pressure, after which filters were freeze dried and stored at −20 °C until analysis. The carbon and nitrogen compositions, and isotopic ratio ($^{13}C/^{12}C$ or $^{15}N/^{14}N$), of dried POM and macrophyte samples were determined at the UC Davis Stable Isotope Facility and reported in standard delta notation ($\delta^{13}C$ or $\delta^{15}N$), defined as parts per thousand (‰) deviation from a standard (Vienna PeeDee Belemnite for $\delta^{13}C$ and atmospheric N_2 for $\delta^{15}N$, Peterson and Fry, 1987). The DOC concentrations and isotopic compositions ($\delta^{13}C$-DOC) were determined using an EA-IRMS analyzer following the protocol of Alberic (2011). The DIC isotopic compositions ($\delta^{13}C$-DIC) were also determined using an EA-IRMS analyzer following the protocol of Bouillon et al. (2007). However, DIC concentrations were not measured, as microcosms were continuously aerated with pumps. The concentration of nitrites (NO_2^-), nitrates (NO_3^-) and ammonium (NH_4^+) dissolved fractions, summarized as DIN (dissolved inorganic nitrogen), as well as orthophosphate concentrations (PO_4^{3-}) were determined by spectrophotometry following a modified method of Grasshoff et al. (1999). Total bacterial abundances were determined by direct epifluorescence microscopy counting, using 4,6-diamidino-2-phenyl-indole (DAPI) up to a final concentration of 1 μg mL^{-1} after 15 min of incubation (Porter and Feig, 1980). Direct counts were performed at 1250x magnification, under an epifluorescence microscope (Leica Leitz DMR; 365 nm). In turbid samples (high suspended matter content), subsamples were pre-treated (before staining) by addition of 150 μl of Tween, sonicated at 35 khz for 5 min, and centrifuged at 3000*g* during 10 min at 4 °C (Chevaldonne and Godfroy, 1997; Hubas et al., 2007a,b).

2.4. Data analysis

The data obtained for each microcosm were compared, to evidence variations between treatments. All FA of POM (up to 40) were used in these analyzes without transformation and were represented by their relative proportions. A dissimilarity matrix between each pair of samples was calculated using the Bray-Curtis index. Dissimilarities between samples were then graphically represented using an nMDS (non-metric MultiDimensional Scaling, Zuur et al., 2007). Differences between groups were tested using analyzes of similarities tests (ANOSIM, Oksanen et al., 2010), without considering temporal variability. When differences were significant, a similarity percentages analysis (SIMPER, Oksanen et al., 2010) was used to determine the relative contribution of each FA to differences between two groups.

The differences in the isotopic compositions ($\delta^{13}C$-DOC, $\delta^{13}C$-POC, $\delta^{15}N$-PON and $\delta^{13}C$-DIC) as well as differences in POC, DOC, DIN, PO_4^{3-} concentrations and bacterial abundance between treatments (n = 5) were tested using a non-parametric Kruskal-Wallis test (KW). Non-parametric Mann-Whitney-Wilcoxon (MWW) Post-Hoc tests were then used to identify the differences between individual treatments, after correction following a Benjamini and Hochberg (BH) procedure for multiple comparisons (Benjamini and Hochberg, 1995).

The relative contribution of C_4 macrophytes to POM was calculated using a two end member mixing model (Forsberg et al., 1993):

$$\%C_4 = \left[1 - \frac{\delta^{13}C_{source} - \delta^{13}C_{C_4}}{\delta^{13}C_{T_0} - \delta^{13}C_{C_4}}\right] \times 100 \quad (1)$$

where $\delta^{13}C_{source}$ was the $\delta^{13}C$-POC compositions for each time and treatment, $\delta^{13}C_{C_4}$ was the mean *P. repens* composition, $\delta^{13}C_{T_0}$ was the mean POM composition at the beginning of the experiment and % C_4 the *P. repens* contribution to the isotopic compositions of OM in each sample.

All statistical analyzes were implemented within the R programming environment (R Development Core Team 2010, package Vegan, Oksanen et al., 2010), with the probability α set at 0.05.

3. Results

Among macrophyte samples, 41 FA were identified (Table 1) with an intragroup similarity of 92.5 and 93.2% within *P. repens* and *S. auriculata*, respectively, at the beginning of the experiment. *P. repens* was ^{13}C and ^{15}N enriched compared to *S. auriculata* (Table 1).

The water collected in the várzea was characterized by 37 FA (Table 1), where saturated 14:0, 15:0, 16:0 and 18:0 accounted for 70% of the total FA composition of POM. The POC and DOC concentrations were respectively of 1.3 ± 0.1 and 2.8 ± 0.3 mg L^{-1} (Fig. 3), with a carbon isotopic composition of −30.1 ± 0.4‰ for POC and −28.7 ± 0.4‰ for DOC (Fig. 4). DIC was ^{13}C enriched relative to POC and DOC ($\delta^{13}C$-DIC of −11.9 ± 0.2‰, Fig. 4).

Water from the five treatments showed significant differences in their global FA compositions (ANOSIM, R = 0.35, $p < 0.001$, Fig. 2). Samples from Ctrl, SA-LB, SA-HB, and PR-LB had a similar FA composition but differed from samples of PR-HB (Table 2). Similarities in the FA composition within each treatment were higher than 77% (Table 3). A higher proportion of branched FA (mainly 15:0iso and 15:0anteiso) and a lower proportion of 18:0 were observed in PR-HB compared to other treatments (Table 3). The concentrations of

Table 1
FA concentrations and stable isotope compositions ($\delta^{13}C$ and $\delta^{15}N$) of POM (FA: $\mu g\,L^{-1}$) and macrophytes (FA: $mg\,g^{-1}$) collected in Camaleão várzea. In bold are the proportion of saturated (SFA), branched (BFA), monounsaturated (MUFA), polyunsaturated (PUFA) and long chain FA (LCFA).

	POM ($\mu g\,L^{-1}$)			P. repens ($mg\,g^{-1}$)			S. auriculata ($mg\,g^{-1}$)		
FA	n = 3	±	S.D.	n = 3	±	S.D.	n = 3	±	S.D.
12:0	2.25	±	1.81	0.1	±	0.02	0.03	±	$7\,10^{-3}$
13:0	0.39	±	0.1	$1\,10^{-3}$	±	$5\,10^{-4}$	$5\,10^{-3}$	±	$1\,10^{-3}$
14:0	6.13	±	1.61	0.1	±	$4\,10^{-3}$	0.2	±	0.05
15:0	2.25	±	0.34	0.03	±	$2\,10^{-3}$	0.06	±	0.01
16:0	24.14	±	3.95	3.69	±	0.38	2.33	±	0.28
17:0	0.75	±	0.1	0.11	±	0.01	0.05	±	0.01
18:0	5.54	±	1.83	0.74	±	0.12	0.22	±	0.05
19:0	0.31	±	0.02	$4\,10^{-3}$	±	2 10−3	$7\,10^{-3}$	±	$1\,10^{-3}$
20:0	0.3	±	0.09	0.19	±	0.03	0.02	±	$5\,10^{-3}$
22:0	0.38	±	0.14	0.37	±	0.07	0.04	±	$4\,10^{-3}$
%SFA	**78.84**	±	**1.76**	**43.77**	±	**4.67**	**80.35**	±	**3.23**
14:0iso	0.55	±	0.13	0.08	±	0.02	$2\,10^{-3}$	±	$1\,10^{-3}$
15:0anteiso	0.78	±	0.15	0.05	±	0.02	0.01	±	$1\,10^{-3}$
15:0iso	2.67	±	0.68	0.06	±	0.02	0.07	±	$5\,10^{-3}$
16:0iso	0.49	±	0.12	$4\,10^{-3}$	±	$2\,10^{-3}$	0.02	±	$3\,10^{-3}$
17:0anteiso	0.58	±	0.18	$3\,10^{-3}$	±	$8\,10^{-4}$	0.01	±	$2\,10^{-3}$
17:0iso	0.56	±	0.13	0.21	±	0.04	0.04	±	0.01
%BFA	**10.43**	±	**0.76**	**3.23**	±	**0.1**	**3.98**	±	**0.18**
16:1ω5	0.22	±	0.03	0.01	±	$4\,10^{-3}$	0.02	±	$6\,10^{-4}$
16:1ω7	0.36	±	0.32	0.02	±	$5\,10^{-3}$	0.01	±	0.02
16:1ω9	0.13	±	0.07	0.28	±	0.11	$4\,10^{-3}$	±	$3\,10^{-3}$
17:1	0.16	±	0.06	0.01	±	0.01	0.01	±	$2\,10^{-3}$
18:1ω5	0.03	±	0	n.d.	±	n.d.	n.d.	±	n.d.
18:1ω7	0.1	±	0.04	0.06	±	0.01	$5\,10^{-3}$	±	$6\,10^{-4}$
18:1ω9	0.01	±	0.01	n.d.	±	n.d.	n.d.	±	n.d.
18:1ω9	n.d.	±	n.d.	0.21	±	0.04	$2\,10^{-3}$	±	$2\,10^{-3}$
20:1ω11	n.d.	±	n.d.	$2\,10^{-3}$	±	$5\,10^{-4}$	n.d.	±	n.d.
20:1ω9	n.d.	±	n.d.	$8\,10^{-3}$	±	$3\,10^{-3}$	n.d.	±	n.d.
%MUFA	**1.83**	±	**0.35**	**4.79**	±	**0.66**	**1.3**	±	**0.07**
16:4ω3	n.d.	±	n.d.	0.12	±	0.02	0.01	±	$4\,10^{-3}$
18:2ω6	0.1	±	0.08	1.34	±	0.38	$2\,10^{-3}$	±	$9\,10^{-4}$
18:3ω3	0.12	±	0.01	3.6	±	1.07	0.01	±	$4\,10^{-3}$
18:3ω6	0.11	±	0.06	$4\,10^{-3}$	±	$1\,10^{-3}$	0.08	±	0.07
18:4ω3	n.d.	±	n.d.	n.d.	±	n.d.	$1\,10^{-3}$	±	$2\,10^{-3}$
20:2	0.13	±	0.03	0.01	±	$4\,10^{-3}$	$4\,10^{-3}$	±	$2\,10^{-3}$
20:3ω3	0.54	±	0.26	0.03	±	0	0.01	±	$6\,10^{-3}$
20:3ω6	0.31	±	0.1	0.01	±	$1\,10^{-3}$	0.04	±	0.03
20:4ω3	0.34	±	0.05	n.d.	±	n.d.	$3\,10^{-3}$	±	$8\,10^{-4}$
20:4ω6	0.08	±	0.02	0.02	±	$2\,10^{-3}$	$3\,10^{-3}$	±	$8\,10^{-4}$
20:5ω3	0.08	±	0.01	$4\,10^{-3}$	±	$2\,10^{-4}$	$9\,10^{-4}$	±	$3\,10^{-4}$
22:5ω3	0.1	±	0.04	$4\,10^{-3}$	±	$1\,10^{-3}$	$3\,10^{-3}$	±	$1\,10^{-4}$
22:5ω6	2.22	±	0.43	0.04	±	$6\,10^{-3}$	0.05	±	0.01
22:6ω3	0.39	±	0.13	0.01	±	$6\,10^{-4}$	n.d.	±	n.d.
%PUFA	**8.61**	±	**1.67**	**41.57**	±	**4.45**	**5.68**	±	**2.4**
24:0	0.05	±	$7\,10^{-3}$	0.55	±	0.11	0.2	±	0.04
25:0	0.12	±	0.01	0.04	±	$5\,10^{-3}$	0.02	±	$6\,10^{-3}$
26:0	n.d.	±	n.d.	0.23	±	0.06	0.1	±	0.03
%LCFA	**0.28**	±	**0.02**	**6.65**	±	**0.57**	**8.69**	±	**0.91**
$\delta^{13}C$ (‰)	−30.15	±	0.43	−13.02	±	0.81	−30.53	±	0.51
$\delta^{15}N$ (‰)	2.43	±	0.71	4.01	±	1.32	2.25	±	1.11

n.d. = not detected.

Table 2
Summary of ANOSIM pairwise tests for FA composition of POM between treatments. Values in italics ($R < 0.3$) are for high intragroup variability.

Groups	*R*	*p* value
PR-HB: Ctrl	0.80	$<10^{-3}$
PR-HB: PR-LB	0.73	$<10^{-3}$
PR-HB: SA-HB	0.75	$<10^{-3}$
PR-HB: SA-LB	0.82	$<10^{-3}$
PR-LB: Ctrl	*0.27*	$<10^{-3}$
PR-LB: SA-HB	*0.07*	0.06^{NS}
PR-LB: SA-LB	*0.11*	$<10^{-3}$
SA-HB: Ctrl	*0.04*	0.15^{NS}
SA-HB: SA-LB	*0.04*	0.11^{NS}
SA-LB: Ctrl	*0.15*	0.01

NS = non-significant.

POC, DOC, DIN, PO_4^{3-} as well as $\delta^{13}C$-POC, $\delta^{13}C$-DOC, $\delta^{13}C$-DIC and bacterial abundance displayed significant differences between treatments (KW, $p < 0.001$, Table 4, Figs. 3–5), whereas $\delta^{15}N$-PON was similar between all treatments (KW, $p = 0.73$).

The highest concentrations of POC, DOC, DIN, PO_4^{3-} and highest bacterial abundance, were observed in PR-HB (Figs. 3 & 5, Table 4). However, a higher POC concentration was recorded in SA-HB compared to PR-LB and SA-LB (Table 4, Fig. 3). No differences in DOC concentration were observed between SA-HB, PR-LB and Ctrl, whereas SA-LB displayed the lowest DOC concentration. In contrast, the $\delta^{13}C$-POC was significantly higher in PR-HB (-14.3 ± 1.0‰) and in PR-LB (-21.0 ± 3.1‰) compared to other treatments (Fig. 4, Table 4). However, no difference was found between the isotopic compositions of SA and Ctrl treatments (MWW, $p > 0.05$, Table 4). The contribution of *P. repens* to the ^{13}C enrichment recorded in POC from PR-HB and PR-LB reached 94.2 and 63.2%, respectively (Fig. 4, Eq. (1)). Similarly, the highest $\delta^{13}C$-DOC was recorded in

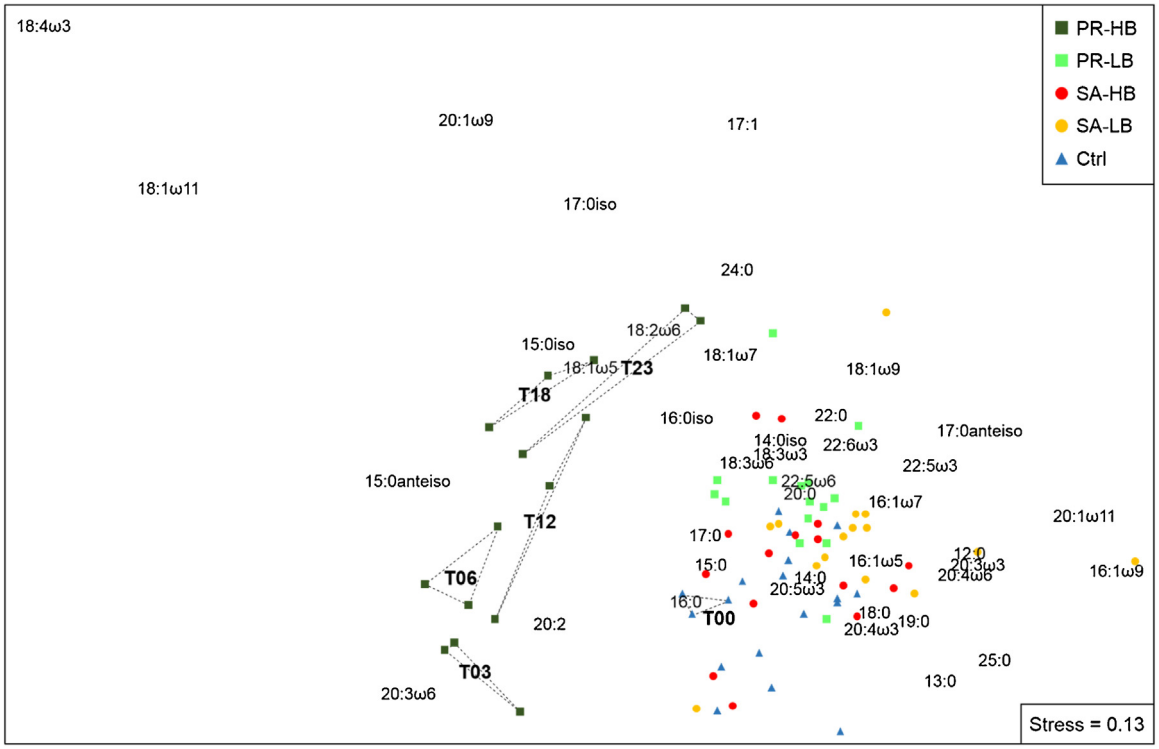

Fig. 2. Nonmetric MDS of FA proportions (%) in POM. Squares (■) are for *P. repens* treatments with high (dark green) and low (light green) biomasses, circles (●) are for *S. auriculata* treatments with high (red) and low (orange) biomasses and blue triangles (▲) are for the Ctrl treatment (for interpretation of the references to colour in this figure legend, the reader is referred to the web version of this article.)

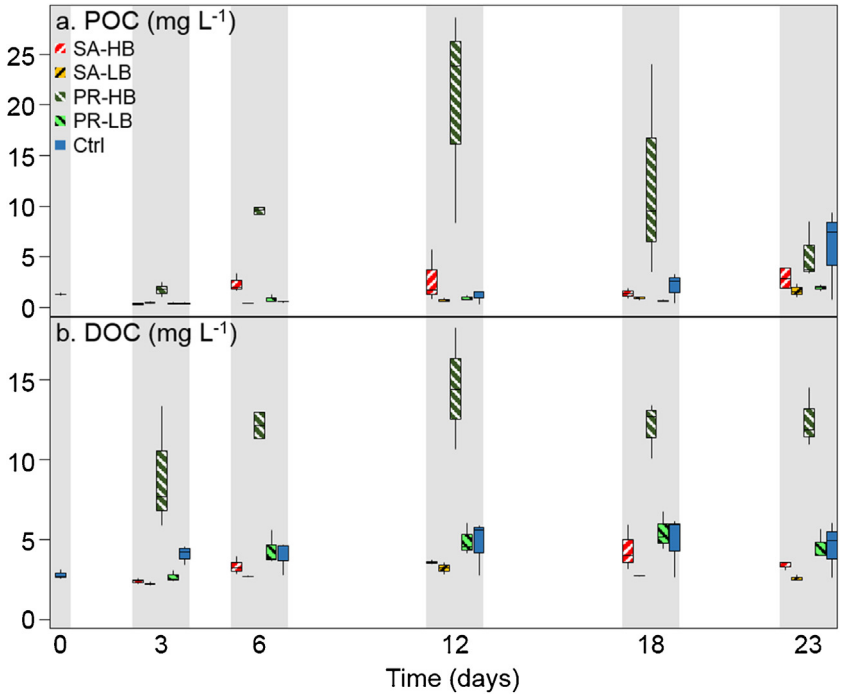

Fig. 3. Boxplot of POC (a.) and DOC (b.) concentrations in each treatment: PR-HB (dark green), PR-LB (light green), SA-HB (red), SA-LB (orange) and Ctrl (blue). Note that DIC time-courses were not determined because of the CO_2 loss to the atmosphere occurring throughout the experiment (for interpretation of the references to colour in this figure legend, the reader is referred to the web version of this article.)

PR-HB (-17.8 ± 1.2‰) with a contribution of *P. repens* to the DOC of 70.7% (Fig. 4, Eq. (1)). A higher δ^{13}C-DOC was also observed in PR-LB (-24.9 ± 1.0‰, Fig. 4, Table 4) compared to SA-HB and SA-LB, with a contribution of *P. repens* to the DOC reaching 27.8%. A significant increase in δ^{13}C-DIC was only recorded for PR-HB (-5.9 ± 2.9‰, Fig. 4, Table 4), concomitantly to a decrease in δ^{13}C-DIC for SA-HB (-17.8 ± 3.7‰, Fig. 4, Table 4). In contrast, no differences were found between the Ctrl with both SA and PR low biomass treatments (MWW, $p > 0.05$, Table 4). δ^{13}C of organic and inorganic

Table 3
Intragroup similarity of FA compositions in different treatments, and percentages of FA explaining most of this similarity (SIMPER procedure).

Treatment (intragroup similarity)	14:0	15:0iso	15:0anteiso	15:0	16:0	18:0	22:5ω6	Σ (%)
PR-HB (77.3%)	6.5	11.2	6.3	3.9	44.1	4.9	5.1	76.8
PR-LB (85.1%)	8.7	6.8	1.6	3.7	33.7	12.7	4.5	73.7
SA-HB (82.6%)	8.8	3.9	1.5	3.4	37.1	13.8	5.0	75.4
SA-LB (81.7%)	9.4	3.4	1.4	3.5	33.0	13.2	4.0	71.7
Ctrl (83.7%)	8.5	3.8	1.4	3.3	39.4	14.3	4.9	77.7

Table 4
Summary of KW and MWW pairwise tests for δ^{13}C-POC, δ^{13}C-DOC, δ^{13}C-DIC; POC, DOC, DIN, PO_4^{3-} concentrations and bacterial abundances of water samples between treatments.

	δ^{13}C-POC	δ^{13}C-DOC	δ^{13}C-DIC	[POC]	[DOC]	[DIN]	[PO_4^{3-}]	Bact
KW Global test	$5\ 10^{-7}$	$3\ 10^{-8}$	$6\ 10^{-9}$	$5\ 10^{-6}$	$4\ 10^{-6}$	10^{-5}	10^{-6}	10^{-9}
PR-HB: Ctrl	$7\ 10^{-4}$	$3\ 10^{-4}$	$8\ 10^{-4}$	$1\ 10^{-3}$	$1\ 10^{-3}$	$1\ 10^{-3}$	$2\ 10^{-3}$	$<10^{-4}$
PR-HB: PR-LB	$7\ 10^{-4}$	$1\ 10^{-3}$	0.03	$1\ 10^{-4}$	$1\ 10^{-3}$	0.05	$5\ 10^{-3}$	$<10^{-4}$
PR-HB: SA-HB	$7\ 10^{-4}$	$2\ 10^{-4}$	$<10^{-4}$	$7\ 10^{-3}$	$1\ 10^{-3}$	$4\ 10^{-3}$	$2\ 10^{-3}$	$<10^{-4}$
PR-HB: SA-LB	$7\ 10^{-4}$	$2\ 10^{-4}$	$9\ 10^{-3}$	$1\ 10^{-4}$	$2\ 10^{-4}$	$4\ 10^{-3}$	$2\ 10^{-3}$	$<10^{-4}$
PR-LB: Ctrl	$9\ 10^{-4}$	$3\ 10^{-4}$	0.44^{NS}	0.86^{NS}	0.71^{NS}	$2\ 10^{-3}$	0.07^{NS}	0.15^{NS}
PR-LB: SA-HB	$7\ 10^{-4}$	$2\ 10^{-4}$	$<10^{-4}$	0.05	0.06^{NS}	0.09^{NS}	0.06^{NS}	0.06^{NS}
PR-LB: SA-LB	$7\ 10^{-4}$	$2\ 10^{-4}$	0.59^{NS}	0.64^{NS}	$2\ 10^{-3}$	0.13^{NS}	0.06^{NS}	0.01
SA-HB: Ctrl	0.60^{NS}	0.23^{NS}	$<10^{-4}$	0.29^{NS}	0.11^{NS}	0.06^{NS}	0.90^{NS}	0.33^{NS}
SA-HB: SA-LB	0.11^{NS}	0.94^{NS}	$<10^{-4}$	0.03	0.02	0.46^{NS}	0.90^{NS}	0.12^{NS}
SA-LB: Ctrl	0.08^{NS}	0.25^{NS}	0.38^{NS}	0.58^{NS}	$2\ 10^{-3}$	$1\ 10^{-3}$	0.90^{NS}	0.04

NS = non-significant.

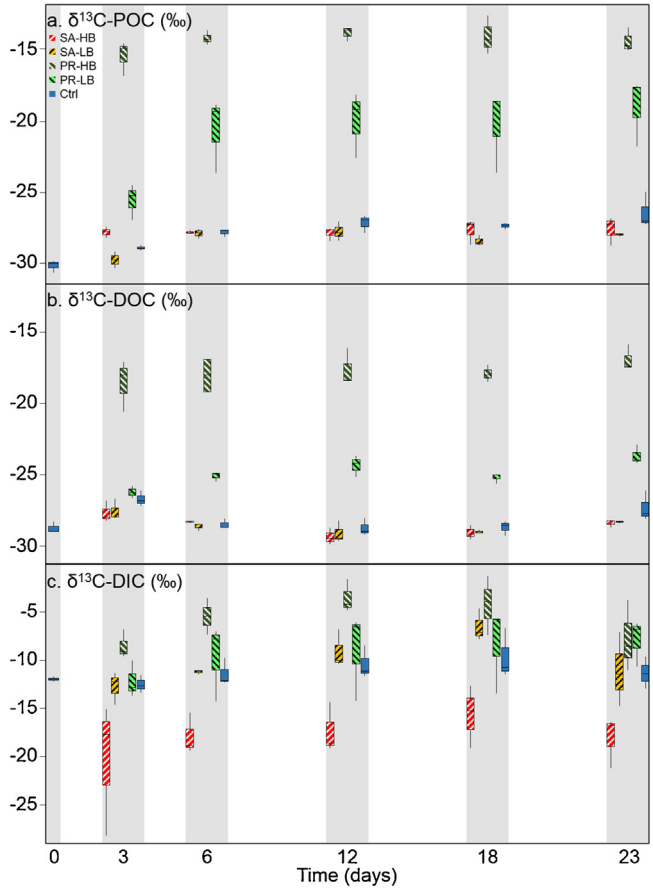

Fig. 4. Boxplot of δ^{13}C-POC (a.), δ^{13}C-DOC (b.) δ^{13}C-DIC (c.) in each treatment: PR-HB (dark green), PR-LB (light green), SA-HB (red), SA-LB (orange) and Ctrl (blue) (for interpretation of the references to colour in this figure legend, the reader is referred to the web version of this article.)

matters increased after 3 to 6 days in PR treatments, whereas no temporal trends were recorded for Ctrl and SA treatments except for δ^{13}C-DIC of SA-HB (Fig. 4).

4. Discussion

The present microcosm experiment highlights significantly different degradation patterns of two C_3 and C_4 Amazon macrophytes. Over a 23 day experiment, our results revealed a major impact of *P. repens* degradation, at high biomass, on OM composition. This impact was apparently related to the biomass of macrophytes used in the experiment as well as to the inherent biodegradability of C_4 compared to C_3 macrophytes. Indeed, even though the fast degradation of the C_4 macrophyte was most evident in PR-HB, as revealed by all measured parameters, it was also observed in the PR-LB. For instance, PR-LB treatments (25 g of fresh macrophytes in a 60 L tank) showed stronger ^{13}C enrichment in POC and DOC than SA-HB (100 g of macrophytes in a 60 L tank). There was however a slight increase in POC concentrations as well as a decrease in δ^{13}C-DIC in the *S. auriculata* high biomass treatments that reveals on-going degradation.

In this experiment, *P. repens* displayed large proportions of 18:2ω6 and 18:3ω3 polyunsaturated FA (up to 44% of total FA), which is consistent with previous characterization of this FA as markers of macrophytes in this environment (Mortillaro et al., 2011). Similarly, carbon stable isotope compositions of both *P. repens* and *S. auriculata* were consistent with those expected from plants with C_4 and C_3 photosynthetic pathways (-13.0 ± 0.8 and -30.5 ± 0.5‰, respectively, Smith and Epstein, 1971).

4.1. *Contribution of* P. repens *(C_4) and* S. auriculata *(C_3) to POM*

In PR treatments, POC was significantly enriched in ^{13}C, which indicates a contribution of *P. repens*, after its hydrolysis into the POM pool. This contribution was estimated to reach 94.2 and 63.2% of total POM composition for PR-HB and PR-LB, respectively, using a two-end-member mixing model. This was surprising as previous studies, characterizing POM in the Amazon Basin, suggested a low contribution of C_4 macrophytes (Hedges et al., 1986; Mortillaro et al., 2011; Moreira-Turcq et al., 2013). The contribution of *P. repens* to POM was confirmed by the increased proportion of branched FA in PR treatments (15:0iso and 15:0anteiso). These FA are regularly described as biomarkers of bacteria (Volkman et al., 1980; Kaneda, 1991; Mfilinge et al., 2003) and suggest here that in addition to hydrolysis, *P. repens* leaves were decomposed by heterotrophic

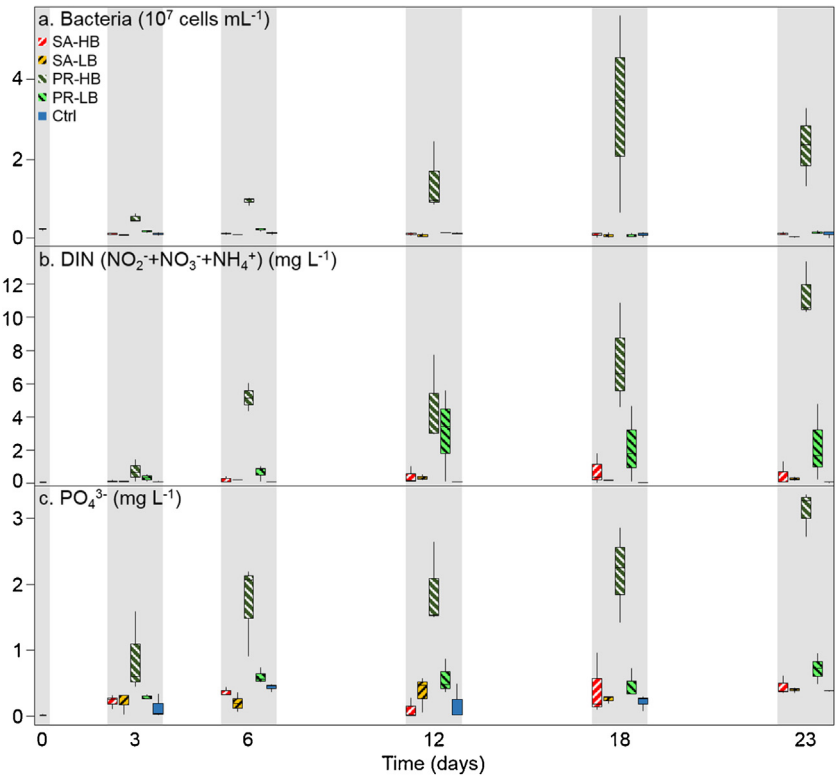

Fig. 5. Boxplot of bacteria abundances (a.), DIN (b.) and PO_4 (c.) concentrations in each treatment: PR-HB (dark green), PR-LB (light green), SA-HB (red), SA-LB (orange) and Ctrl (blue) (for interpretation of the references to colour in this figure legend, the reader is referred to the web version of this article.)

microbial communities. Indeed, the transfer of FA to POM, including branched FA, was previously recorded from decomposing mangroves (Mfilinge et al., 2003). Similarly, the transfer of FA and the ^{13}C enrichment of POM and sediments were evidenced in salt-marsh from the decomposition of the C_4 *Spartina* spp. (Boschker et al., 1999). In salt-marsh ecosystems, the composition of POM affected by *Spartina* spp. decomposition changed from predominantly unsaturated to branched and saturated FA typical of bacteria (Johnson and Calder, 1973; Schultz and Quinn, 1973). Similar findings were reported in PR-HB and differences in FA compositions and ^{13}C enrichments reported for OM between PR and Ctrl treatments occurred in the first 3–6 days of the experiment. These changes in OM composition, as well as high bacterial abundance recorded in PR-HB, suggest a fast decomposition of this macrophyte, which may have exceeded hydrolysis (in agreement with previous studies; Fellerhoff et al., 2003).

Contrastingly to *P. repens*, no differences were reported between SA and Ctrl treatments for FA and $\delta^{13}C$-POC. Yet, decomposition of *S. auriculata* could not be excluded using $\delta^{13}C$-POC analyses. Indeed, fresh leaves of *S. auriculata* (-30.5 ± 0.5‰) had a similar composition to POM (-30.1 ± 0.4‰) at the beginning of the experiment. However, the higher POC concentrations measured in SA-HB compared to PR-LB and SA-LB suggest an effective hydrolysis of this macrophyte. The lack of differences between SA and Ctrl treatments for FA compositions and $\delta^{13}C$-POC suggest however a slower hydrolysis of *S. auriculata* compared to *P. repens*. Indeed, Howard-Williams and Junk (1976) recovered 50% of *S. auriculata* initial dry weight at the end of a 186 days decomposition experiment. Similarly, Fellerhoff et al. (2003) recovered 80% of *S. auriculata* initial dry weight after 21 days of incubation. During our experiment, large macrophyte debris were observed for a much longer time in the *S. auriculata* treatments than in the *P. repens* treatments. This higher resistance to fractionation of the C_3 macrophyte was consistent with the differences in FA, POC and $\delta^{13}C$-POC of the fine POM fraction (<200 μm).

4.2. Impact of macrophyte degradation on dissolved compounds

Decomposition of *P. repens* tissues led to a ^{13}C enrichment of DOC and DIC. Such increase of $\delta^{13}C$-DIC resulted from bacterial mineralization of macrophyte organic carbon and CO_2 equilibration at the air/water interface (Quay et al., 1992; Hedges et al., 1994; Mayorga et al., 2005). Because the experiment was performed in contact with air in order to maintain aerobic conditions, the $\delta^{13}C$-DIC signature was affected by isotopic equilibration with the atmosphere. This process tends to slowly increase the $\delta^{13}C$-DIC to a value close to the isotopic equilibrium with the atmosphere at around 0‰ (Polsenaere and Abril, 2012). Consequently, the observed $\delta^{13}C$-DIC values are the result of a balance between the DIC production from the C_3 or C_4 plants decomposition and equilibration with the atmosphere. In SA-HB, the rapid $\delta^{13}C$-DIC decrease from -11.9 ± 0.2‰ at the beginning of the experiment to -20.3 ± 7.0‰ after 3 days of incubation reveals that the C_3 macrophytes were undergoing mineralization processes. Indeed, hydrolysis tends to leach out compounds relatively enriched in ^{13}C with respect to more recalcitrant compounds (e.g. lignin) depleted in ^{13}C (Costantini et al., 2014).

Previous works in the Amazon have attributed ^{13}C enrichment of DIC to the preferential oxidation of organic carbon derived from C_4 macrophytes (Rai and Hill, 1984; Chanton et al., 1989; Quay et al., 1992; Waichman, 1996). Several other studies based on solute distribution suggested that C_4 grasses are more biodegradable than the bulk OM (Hedges et al., 1986; Quay et al., 1992; Mayorga et al., 2005). Ellis et al. (2012) have measured the $\delta^{13}C$ of respired CO_2 in closed incubations at different stages of the hydrological cycle in the Solimões River and concluded that C_3 plants, C_4 plants and phytoplankton, all contributed to respiration in the Amazon River. The

results of our incubations suggest however that high macrophyte biomasses are necessary in order to significantly alter the δ^{13}C-DIC signature locally.

Besides carbon, the nitrogen (N) and phosphorus (P) concentrations in floodplain waters were also affected by the decomposition and mineralization of macrophytes. A large release of PO_4, DIN and potassium (K) was previously evidenced during the decomposition of *P. fasciculatum* (Furch and Junk, 1992). The decomposition of *P. fasciculatum* had the potential to supply floodplains with 242 kg ha^{-1} of N and 66 kg ha^{-1} of P in Furch and Junk (1992) nutrients budget. Following these authors' calculations (i.e. maximum amounts of bio-elements released to water reported to maximum macrophyte biomasses), *P. repens* showed the potential, in our degradation experiment, to supply floodplains with 176.4 kg ha^{-1} of N and 48.2 kg ha^{-1} of P. On the other hand, *S. auriculata* contribution to floodplains is estimated to reach 0.13 kg ha^{-1} of N and 2.44 kg ha^{-1} of P only. Therefore, our study demonstrates that *P. repens* represents a predominant source of N and P.

Fast nutrient recycling from decomposing macrophytes may fertilize Amazon floodplains, where N and P are growth-limiting factors (Devol et al., 1984; Forsberg, 1984; Setaro and Melack, 1984). Within the Amazon Basin, aquatic grasses such as *P. repens* have been suggested to be able of atmospheric N_2 fixation (Martinelli et al., 1992), so that atmospheric N_2 may contribute up to 90% of plant N for stands of *P. repens* (Kern and Darwich, 2003). Therefore, the fast decomposition of N_2 fixing macrophytes may play a predominant role as a natural fertilizer for floodplains (Piedade et al., 1991; Kern and Darwich, 2003), stimulating phytoplankton production during the falling water period, when macrophytes start to decompose (Rai and Hill, 1984).

In Amazon floodplains, *P. repens* maximum biomasses were observed during the wet season (Junk and Piedade, 1993b; Silva et al., 2009), where C_4 macrophyte contribution to the primary production in várzea was estimated to reach 65% (Melack and Forsberg, 2001). During this season, POC and DOC mainly originate from depleted carbon sources similar to C_3 primary producers (Hedges et al., 1994; Mortillaro et al., 2011). However during the dry season, macrophytes are subject to intensive degradation as water level decreases (Engle et al., 2008). An increasing contribution of macrophytes to OM composition, due to the accumulation of plant detritus, was suggested in the Amazon várzea (Mortillaro et al., 2011). However, although macrophytes have been demonstrated experimentally to affect the δ^{13}C-POC and δ^{13}C-DOC, fast microbial mineralization of organic carbon suggests that only large macrophyte biomasses, produced during the flood season, have the potential to affect δ^{13}C-POC and δ^{13}C-DOC within floodplains. Indeed, C_4 material may contribute to sediments OM composition (Sobrinho et al., 2016) according to spatial variability in C_4 macrophytes (Hess et al., 2003), despite a low burial of organic carbon in floodplain sediments (Moreira-Turcq et al., 2004). Therefore, most C_4 macrophytes are mineralized (Piedade et al., 1991; Junk and Piedade, 1993a) and thus contribute significantly to CO_2 outgassing, as previously suggested (Quay et al., 1992). Moreover, bacterial growth has been shown, within Amazon floodplains, to display a low efficiency (Vidal et al., 2015). This low efficiency implies, besides high respiration rates, a low transfer of C_4 carbon to higher trophic levels. The production of C_3 macrophytes within the central Amazon Basin is much more limited than C_4 macrophytes (Furch and Junk, 1992). However, the lower lability of these macrophyte debris compared to C_4 macrophyte debris makes them available for being channeled through aquatic food webs. These findings can explain why Amazon food webs are mainly centered on a C_3 carbon source (Araujo-Lima et al., 1986; Hamilton et al., 1992; Forsberg et al., 1993), although C_4 macrophytes display a greater food quality and biomass for specialized herbivore fish species (Mortillaro et al., 2015).

5. Conclusion

Within the present experiment, the higher lability of C_4 compared to C_3 macrophytes was demonstrated. The contribution of *P. repens* to POC and DOC isotopes compositions reached a maximum after 3–6 days, indicating a fast decomposition rate of this macrophyte. Moreover, *P. repens* biomasses had a noticeable impact on OM composition. The decomposition of C_4 macrophytes was followed by the mineralization into DIC, as suggested by δ^{13}C-DIC, as well as by the release of DIN and P. Therefore, the fast mineralization of C_4 macrophytes, as well as the natural mixing of POM with ^{13}C-depleted primary producers (e.g. phytoplankton, C_3 macrophytes, periphyton, and trees), should account for the overall low contribution of C_4 carbon sources to the central Amazon aquatic food webs.

Acknowledgments

This research is a contribution to the CARBAMA project, supported by the ANR (French National Agency for Research, grant number 08-BLAN-0221), and the CNPq (National Council for Scientific and Technological Development—Brazil, Universal Program grant number 477655/2010-6); it was conducted within an international cooperation agreement between the CNPq (Brazil) and the IRD (Institute for Research and Development—France), and under the auspices of the Environmental Research Observatory Hydrology and Geochemistry of the Amazon Basin (HYBAM), supported by the INSU and the IRD. We are grateful to Jessica Chicheportiche (LOG laboratory) for bacterial abundance estimations. We also want to thanks two anonymous reviewers whose comments helped improve this manuscript.

References

Abril, G., Martinez, J.M., Artigas, L.F., Moreira-Turcq, P., Benedetti, M.F., Vidal, L., Meziane, T., Kim, J.H., Bernardes, M.C., Savoye, N., Deborde, J., Souza, E.L., Alberic, P., Landim de Souza, M.F., Roland, F., 2014. Amazon river carbon dioxide outgassing fuelled by wetlands. Nature 505, 395–398.

Alberic, P., 2011. Liquid chromatography/mass spectrometry stable isotope analysis of dissolved organic carbon in stream and soil waters. Rapid Commun. Mass Spectrom. 25, 3012–3018.

Araujo-Lima, C.A.R.M., Forsberg, B.R., Victoria, R., Martinelli, L., 1986. Energy sources for detritivorous fishes in the Amazon. Science 234, 1256–1258.

Benjamini, Y., Hochberg, Y., 1995. Controlling the false discovery rate: a practical and powerfull approach to multiple testing. J. R. Stat. Soc. Ser. B-Methodol. 57, 289–300.

Bligh, E.G., Dyer, W.J., 1959. A rapid method of total lipid extraction and purification. Can. J. Biochem. Physiol. 37, 911–917.

Boschker, H.T.S., de Brouwer, J.F.C., Cappenberg, T.E., 1999. The contribution of macrophyte-derived organic matter to microbial biomass in salt-marsh sediments: stable carbon isotope analysis of microbial biomarkers. Limnol. Oceanogr. 44, 309–319.

Bouillon, S., Middelburg, J.J., Dehairs, F., Borges, A.V., Abril, G., Flindt, M.R., Ulomi, S., Kristensen, E., 2007. Importance of intertidal sediment processes and porewater exchange on the water column biogeochemistry in a pristine mangrove creek (Ras Dege, Tanzania). Biogeosciences 4, 311–322.

Chanton, J., Crill, P., Bartlett, K., Martens, C., 1989. Amazon capims (floating grassmats): a source of ^{13}C enriched methane to the troposphere. Geophys. Res. Lett. 16, 799–802.

Chevaldonne, P., Godfroy, A., 1997. Enumeration of microorganisms from deep-sea hydrothermal chimney samples. FEMS Microbiol. Lett. 146, 211–216.

Costantini, M.L., Calizza, E., Rossi, L., 2014. Stable isotope variation during fungal colonisation of leaf detritus in aquatic environments. Fungal Ecol. 11, 154–163.

Devol, A.H., Dossantos, A., Forsberg, B.R., Zaret, T.M., 1984. Nutrient addition experiments in Lago Jacaretinga, Central Amazon, Brazil: 2. The effect of humic and fluvic acids. Hydrobiologia 109, 97–103.

Ellis, E.E., Richey, J.E., Aufdenkampe, A.K., Krusche, A.V., Quay, P.D., Salimon, C., da Cunha, H.B., 2012. Factors controlling water-column respiration in rivers of the central and southwestern Amazon basin. Limnol. Oceanogr. 57, 527–540.

Engle, D.L., Melack, J.M., 1993. Consequences of riverine flooding for seston and the periphyton of floating meadows in an Amazon floodplain lake. Limnol. Oceanogr. 38, 1500–1520.
Engle, D.L., Melack, J.M., Doyle, R.D., Fisher, T.R., 2008. High rates of net primary production and turnover of floating grasses on the Amazon floodplain: implications for aquatic respiration and regional CO2 flux. Glob. Change Biol. 14, 369–381.
Fellerhoff, C., Voss, M., Wantzen, K.M., 2003. Stable carbon and nitrogen isotope signatures of decomposing tropical macrophytes. Aquat. Ecol. 37, 361–375.
Forsberg, B.R., Araujo-Lima, C.A.R.M., Martinelli, L.A., Victoria, R.L., Bonassi, J.A., 1993. Autotrophic carbon sources for fish of the central Amazon. Ecology 74, 643–652.
Forsberg, B.R., 1984. Nutrient processing in Amazon floodplain lakes. Verhandlungen der Internationalen Vereinigung für Theoretische und Angewandte Limnologie 22, 1294–1298.
Furch, K., Junk, W., 1992. Nutrient dynamics of submersed decomposing Amazonian herbaceous plant specie: *Paspalum fasciculatum* and *Echinochloa polystachya*. Revue d'Hydrobiologie Tropicale 25, 75–85.
Grasshoff, K., Kremling, K., Ehrhardt, M., 1999. Methods of Seawater Analysis. Wiley-VCH Verlag GmbH, Weinheim, Germany.
Hamilton, S.K., Lewis, W.M., Sippel, S.J., 1992. Energy sources for aquatic animals in the Orinoco river floodplain: evidence from stable isotopes. Oecologia 89, 324–330.
Hedges, J.I., Clark, W.A., Quay, P.D., Richey, J.E., Devol, A.H., Santos, U.D., 1986. Compositions and fluxes of particulate organic material in the Amazon river. Limnol. Oceanogr. 31, 717–738.
Hedges, J.I., Cowie, G.L., Richey, J.E., Quay, P.D., Benner, R., Strom, M., Forsberg, B.R., 1994. Origins and processing of organic matter in the Amazon river as indicated by carbohydrates and amino acids. Limnol. Oceanogr. 39, 743–761.
Hess, L.L., Melack, J.M., Novo, E.M.L.M., Barbosa, C.C.F., Gastil, M., 2003. Dual-season mapping of wetland inundation and vegetation for the central Amazon basin. Remote Sens. Environ. 87, 404–428.
Howard-Williams, C., Junk, W.J., 1976. The decomposition of aquatic macrophytes in the floating meadows of a Central amazonian varzea lake. In: Biogeographica. The Hague, pp. 115–123.
Hubas, C., Artigas, L.F., Davoult, D., 2007a. Role of the bacterial community in the annual benthic metabolism of two contrasted temperate intertidal sites (Roscoff Aber Bay France). Mar. Ecol. Progress Ser. 344, 39–48.
Hubas, C., Lamy, D., Artigas, L.F., Davoult, D., 2007b. Seasonal variability of intertidal bacterial metabolism and growth efficiency in an exposed sandy beach during low tide. Mar. Biol. 151, 41–52.
Johnson, R.W., Calder, J.A., 1973. Early diagenesis of fatty acids and hydrocarbons in a salt-marsh environment. Geochim. Cosmochim. Acta 37, 1943–1955.
Junk, W.J., Howard-Williams, C., 1984. Ecology of aquatic macrophytes in Amazonia. In: Sioli, H. (Ed.), The Amazon, Limnology and Landscape Ecology of a Mighty Tropical River and Its Basin. Junk, Dordrecht, pp. 269–293.
Junk, W.J., Piedade, M.T.F., 1993a. Biomass and primary production of herbaceous plant communities in the Amazon floodplain. Hydrobiologia 263, 155–162.
Junk, W.J., Piedade, M.T.F., 1993b. Herbaceous plants of the Amazon floodplain near Manaus: species diversity and adaptations to the flood pulse. Amazoniana-Limnologia Et Oecologia Regionalis Systemae Fluminis Amazonas 12, 467–484.
Junk, W.J., Piedade, M.F.T., 1997. Plant life in the floodplain with special reference to herbaceous plants. In: Junk, W.J. (Ed.), The Central Amazon Floodplain: Ecology of a Pulsing System. Springer, Berlin Heidelberg New York, pp. 147–185.
Kaneda, T., 1991. Iso-fatty and anteiso-fatty acids in bacteria: biosynthesis, function, and taxonomic significance. Microbiol. Rev. 55, 288–302.
Kern, J., Darwich, A., 2003. The role of periphytic N_2 fixation for stands of macrophytes in the whitewater floodplain (varzea). Amazoniana-Limnologia Et Oecologia Regionalis Systemae Fluminis Amazonas 17, 361–375.
Martinelli, L.A., Victoria, R.L., Trivelin, P.C.O., Devol, A.H., Richey, J.E., 1992. ^{15}N natural abundance in plants of the Amazon River floodplain and potential atmospheric N_2 fixation. Oecologia 90, 591–596.
Mayorga, E., Aufdenkampe, A.K., Masiello, C.A., Krusche, A.V., Hedges, J.I., Quay, P.D., Richey, J.E., Brown, T.A., 2005. Young organic matter as a source of carbon dioxide outgassing from Amazonian rivers. Nature 436, 538–541.
Melack, J.M., Forsberg, B.R., 2001. Biogeochemistry of Amazon floodplain lakes and associated wetlands. In: McClain, M.E., Victoria, R.L., Richey, J.E. (Eds.), The Biogeochemistry of the Amazon Basin. Oxford University Press, New York, pp. 235–274.
Mfilinge, P.L., Meziane, T., Bachok, Z., Tsuchiya, M., 2003. Fatty acids in decomposing mangrove leaves: microbial activity: decay and nutritional quality. Mar. Ecol.-Progress Ser. 265, 97–105.
Moreira-Turcq, P., Bonnet, M.P., Amorim, M., Bernardes, M., Lagane, C., Maurice, L., Perez, M., Seyler, P., 2013. Seasonal variability in concentration, composition, age, and fluxes of particulate organic carbon exchanged between the floodplain and Amazon river. Glob. Biogeochem. Cycles 27, 119–130.
Moreira-Turcq, P., Jouanneau, J.M., Turcq, B., Seyler, P., Weber, O., Guyot, J.L., 2004. Carbon sedimentation at Lago Grande de Curuai: a floodplain lake in the low Amazon region: insights into sedimentation rates. Palaeogeogr. Palaeoclimatol. Palaeoecol. 214, 27–40.
Morison, J.I.L., Piedade, M.T.F., Muller, E., Long, S.P., Junk, W.J., Jones, M.B., 2000. Very high productivity of the C_4 aquatic gras: echinochloa polystachya in the Amazon floodplain confirmed by net ecosystem CO_2 flux measurements. Oecologia 125, 400–411.
Mortillaro, J.M., Abril, G., Moreira-Turc, P., Sobrinho, R., Perez, M., Meziane, T., 2011. Fatty acid and stable isotope ($\delta^{13}C$: $\delta^{15}N$) signatures of particulate organic matter in the lower Amazon river: seasonal contrasts and connectivity between floodplain lakes and the mainstem. Org. Geochem. 42, 1159–1168.
Mortillaro, J.M., Pouilly, M., Wach, M., Freitas, C.E.C., Abril, G., Meziane, T., 2015. Trophic opportunism of central Amazon floodplain fish. Freshwater Biol. 60, 1659–1670.
Oksanen, J., Blanchet, F.G., Kindt, R., Legendre, P., O'Hara, R.B., Simpson, G.L., Solymos, P., Stevens, M.H.H., Wagner, H., 2010. Vegan: Community Ecology Package. R package version 1. 17–12.
Peterson, B.J., Fry, B., 1987. Stable isotopes in ecosystem studies. Annu. Rev. Ecol. Syst. 18, 293–320.
Piedade, M.T.F., Junk, W.J., Long, S.P., 1991. The productivity of the C_4 gras: echinochloa polystachya on the Amazon floodplain. Ecology 72, 1456–1463.
Polsenaere, P., Abril, G., 2012. Modelling CO_2 degassing from small acidic rivers using water pCO_2, DIC and delta C^{13}DIC data. Geochim. Cosmochim. Acta 91, 220–239.
Porter, K.G., Feig, Y.S., 1980. The use of DAPI for identifying and counting aquatic microflora. Limnol. Oceanogr. 25, 943–948.
Quay, P.D., Wilbur, D.O., Richey, J.E., Hedges, J.I., Devol, A.H., Victoria, R., 1992. Carbon cycling in the Amazon river: implications from the ^{13}C compositions of particles and solutes. Limnol. Oceanogr. 37, 857–871.
Rai, H., Hill, G., 1984. Microbiology of amazonian waters. In: Sioli, H. (Ed.), The Amazon, Limnology and Landscape Ecology of a Mighty Tropical River and Its Basin. Junk W., Dordrecht, pp. 413–441.
Schultz, D.M., Quinn, J.G., 1973. Fatty acid composition of organic detritus fro: spartina alterniflora. Estuarine Coastal Mar. Sci. 1, 177–190.
Setaro, F.V., Melack, J.M., 1984. Responses of phytoplankton to experimental nutrient enrichment in an Amazon floodplain lake. Limnol. Oceanogr. 29, 972–984.
Silva, T.S.F., Costa, M.P.F., Melack, J.M., 2009. Annual net primary production of macrophytes in the eastern Amazon floodplain. Wetlands 29, 747–758.
Silva, T.S.F., Melack, J.M., Novo, E., 2013. Responses of aquatic macrophyte cover and productivity to flooding variability on the Amazon floodplain. Glob. Change Biol. 19, 3379–3389.
Smith, B.N., Epstein, S., 1971. Two categories of $^{13}C/^{12}C$ ratios for higher plants. Plant Physiol. 47, 380–384.
Sobrinho, R.L., Bernardes, M.C., Abril, G., Kim, J.H., Zell, C.I., Mortillaro, J.M., Meziane, T., Moreira-Turcq, P., Sinninghe Damsté, J.S., 2016. Spatial and seasonal contrasts of sedimentary organic matter in floodplain lakes of the central Amazon basin. Biogeoscience 13, 467–482.
Volkman, J.K., Johns, R.B., Gillan, F.T., Perry, G.J., Bavor, H.J., 1980. Microbial lipids of an intertidal sediment: 1. Fatty accids and hydrocarbons. Geochim. Cosmochim. Acta 44, 1133–1143.
Vidal, L.O., Abril, G., Artigas, L.F., Melo, M.L., Bernardes, M.C., Lobão, L.M., Reis, M.C., Moreira-Turcq, P., Benedetti, M., Tornisielo, V.L., Roland, F., 2015. Hydrological pulse regulating the bacterial heterotrophic metabolism between Amazonian mainstems and floodplain lakes. Front. Microbiol. 6, 1054.
Waichman, A.V., 1996. Autotrophic carbon sources for heterotrophic bacterioplankton in a floodplain lake of central Amazon. Hydrobiologia 341, 27–36.
Zuur, A.F., Ieno, E.N., Smith, G.M., 2007. Analysing Ecological Data. Springer, Heidelberg, Germany.